NASA's Next Solar Sail: Lessons from NanoSail – D2

Chelsea Katan
Embry-Riddle Aeronautical University
Prescott, AZ, USA, katanc@erau.edu

Faculty Advisor: Dr. David Lanning
Embry-Riddle Aeronautical University

ABSTRACT

NanoSail – D2 unfurled January 17th, 2011 and commenced a nine month Low Earth Orbit path to reentry to evaluate a sail's capacity to deploy in space and deorbit satellites. The orbit was strongly affected by variables including but not limited to: initial attitude, orbit lighting, solar radiation pressure, aerodynamic drag, gravity, and Center of Pressure offsets. The effects of these variables were evaluated through a 3-DOF rigid body simulation. The sail experienced stability in orbits which were continuously lit, i.e. did not orbit behind Earth. Probable drag area experienced by the sail for the mission is also estimated from orbital data and compared to the attitude simulation results. Analysis focuses on sail behavior in full lighting conditions to establish the limits of the sails stability in full lighting. Solar radiation pressure, aerodynamic drag, and gravity torque effects are described. Lastly, a reasonable upper bound on the variation of the Center of Pressure from the geometric center of the sail plane is established. Each of these results contributes to the design requirements for future solar sails.

NOTATION

β	angle between sun-earth line and orbit plane
e	eccentricity
AOP	Argument of Perigee
I	inertia tensor
α	angular attitude [deg]
ω	angular velocity [deg/s]
τ	torque [N m]
ρ	density [kg m^3]
v	velocity [m s^{-1}]
Cd	drag co-efficient
A	drag sail area [m^2]
S	total sail area [m^2]
We	solar constant [J s^{-1} m^{-2}]
c	speed of light in vacuum [m s^{-1}]
r_e	distance of earth from sun [km]
r_s	distance of satellite from sun [km]
k	gravitational constant
R	semi-major axis [km]
I_{xx}	inertial moment about x-axis
I_{yy}	inertial moment about y-axis
I_{zz}	inertial moment about z-axis
a_x	direction cosine of x-axis in body frame
a_y	direction cosine of x-axis in body frame
a_z	direction cosine of x-axis in body frame

1. INTRODUCTION

More than 521,000 human-made defunct devices greater than 1 cm. in diameter now orbit Earth[i]. These objects are represented by the white dots in **Figure 1**[ii] - of which 95% are orbital debris that travel at a velocity of 7-8 km/s and pose an impact danger to operational satellites, space vehicles and the International Space Station. Unless satellites were launched with active deorbit strategies, the devices depend on atmospheric drag to cause the orbit to decay over long periods of time. Solar sails are a potential deorbit solution because they are low mass devices that require little to no fuel to maneuver. Solar sails could deorbit a satellite using solar radiation pressure and/or increased aerodynamic drag.

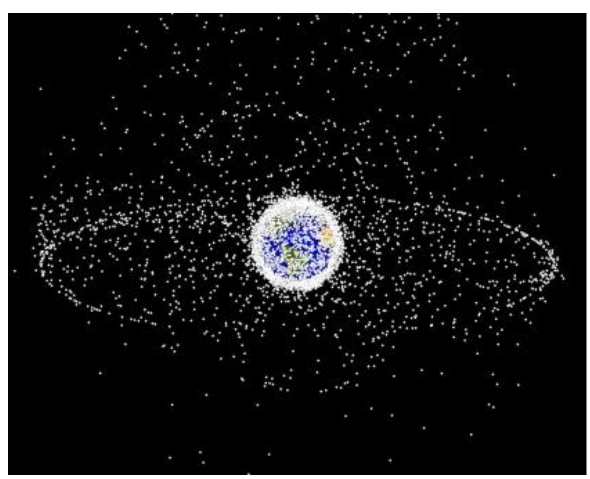

Figure 1. Space Junk Orbiting Earth

Research was conducted to evaluate how the 2011 solar sail NanoSail – D2 (NSD) operated while in orbit. The NSD presented varying drag areas throughout its orbit, thus an effective drag area was ascertained through the use of Satellite Tool Kit (STK) predictions and TLE comparison. Initial attitude effect on the sail's stabilization time and final stabilization attitude were tested. This provides insight to the sail's natural attitude control and stabilization. Three torques affected the sail's orbit: solar radiation pressure, aerodynamic drag, and gravity gradient[iii]. Each torque effect was individually evaluated. The effects of the separate torques on stability are demonstrated in inertial attitude figures and rotation rate figures. The offset of the Center of Pressure (CP) of the sail moved the moment arm of the torques. Thus a trade study was completed to evaluate CP offset effects on stability. This yielded an upper limit of CP offset magnitude for sails of similar structure and Center of Gravity locations.

This research investigates the solar radiation pressure (SRP), aerodynamic drag, and gravity forces that affected NSD's orbital and attitude dynamics. It helps to define the requirements for future solar sail missions, such as deorbiting space junk. Potential orbits and missions will be discussed. Solar, drag, and gravity torque effects on stability will be demonstrated. An upper limit on a solar sail's CP will be established. This data will guide future solar sail design and solar sail mission requirements.

2. BACKGROUND INFORMATION

The objective of NanoSail – D2 (NSD) was to demonstrate sail deployment and de-orbit capability and in doing so raise the Technology Readiness Level (TRL) of solar sails. The satellite was ejected from FASTSAT-HSV01 on January 14, 2011 and the sail unfurled three days later on January 17, 2011. The spacecraft delivered data packages for three days following unfurling. The data consisted of a simple beacon indicating that NSD had deployed and after a few days the batteries died and no further data was available. NSD continued to orbit for 243 days without active controls. Torques from gravity, atmospheric drag and solar radiation pressure determined the attitude of NSD and hence affected the orbit of the sail for the duration of the mission.

Limited orbital data is available for the sail because it delivered data for only three days; and the Two Line Element sets (TLEs) observed by the United States Space Command were not published for NSD. The data sets were obtained through channels at NASA. They included daily observations for the majority of the mission, but excluded the reentry data and a small set of other dates.

The sail was an uncontrolled square sail that expanded from a 3U cube satellite. The X and Y-axes are inertially symmetric and located in the sail plane. The Z-axis of the sail's body frame runs from the sail plane through the cube satellite bus, visible in **Figure 2**[iv]. The sail consisted of four thin triangular sheets of aluminized CP-1 material attached to four Triangular Rollable and Collapsible (TRAC) booms[v]. Each triangle of the sail is mounted to two TRAC boom ends, each 2.2 m. long, and the bus. The sides of the sail are 3.16 m. which produces a sail area of 10 m^2. The TRAC booms shown in **Figure 3** were collapsed inside the cube satellite before launch and deployed the sail in approximately five seconds in space[vi]. The sail deployment demonstrated the boom's stored-strain-energy capacity and structural rigidity, and successfully demonstrated the TRAC technology particularly for future solar sail missions.

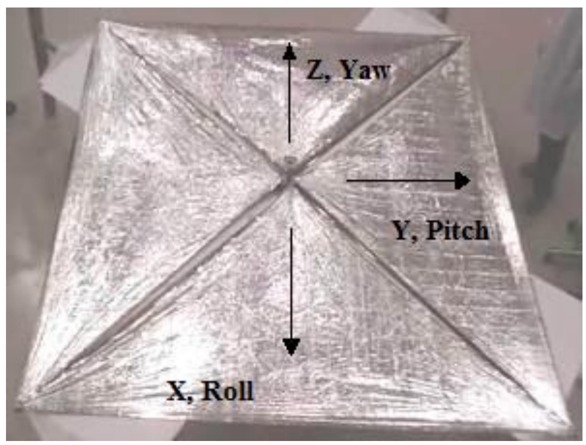

Figure 2: NanoSail - D2 in Ground Deployment Test with Body Axes Labeled

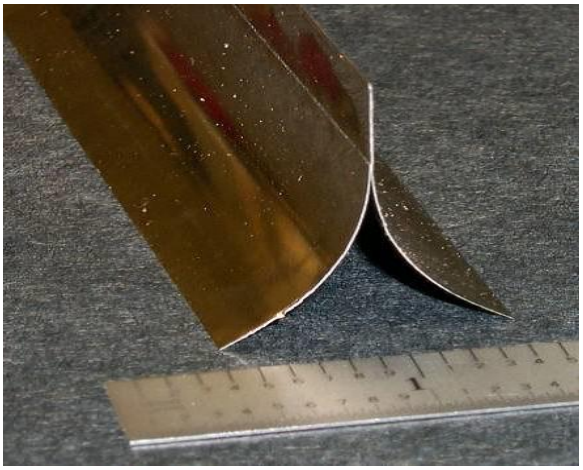

Figure 3. TRAC Boom

Analysis of NanoSail – D2 was challenging because there exists no single software analysis tool that correctly incorporates all forces acting on a solar sail. STK includes accurate models of atmospheric drag forces for known ballistic coefficients and solar radiation effects for spherical objects. Solar Sail Spaceflight Simulation Software (S5) has sufficient models of solar sail behavior in interplanetary travel (which would include SRP and gravity forces) but does not model solar sails in planetary orbits and thus excludes an aerodynamic drag model. STK analysis and a 3-DOF Rigid Body Dynamics model were meshed to properly analyze NanoSail – D2's mission.

3. ANALYSIS

To analyze the solar sail's orbit, full sunlight study periods are most meaningful due to constant solar radiation pressure. β is used as a measure of sunlight exposure over the course of an orbit and is defined as the angle between the sun-earth line and the orbit plane. Maximum or minimum β (±90°) indicates the sail experienced full sun over the course of the orbit. When β = 0° the satellite orbited in Earth's shadow for a segment of each orbit where it experienced aerodynamic drag and gravity but no solar radiation pressure.

At high β angles, solar radiation pressure acts on the sail constantly. SRP most strongly affects eccentricity, *e* and Argument of Perigee, AOP[vii]. To illustrate this concept, STK was used to create predictions of AOP and *e* with and without the spherical model of SRP. In **Figure 4**, AOP comparison, the AOP prediction with SRP shown in red better fits the TLE data shown in blue circles than the AOP prediction without SRP, in green. In the *e* model in **Figure 5**, the eccentricity prediction with spherical SRP model prediction better fits the TLE data than the same prediction without the spherical SRP model.

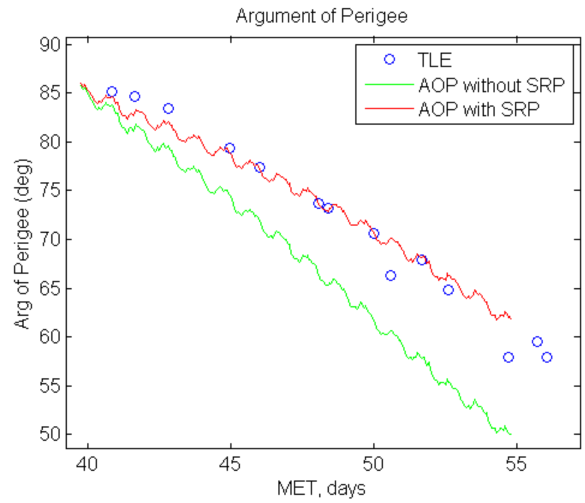

Figure 4. Argument of Perigee Predictions from STK with and without the Spherical SRP Model.

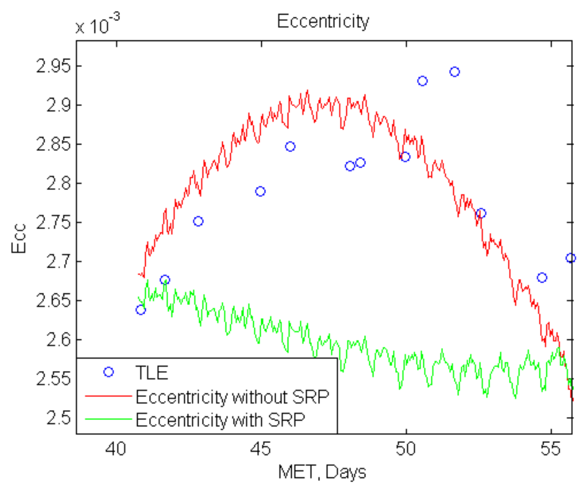

Figure 5. Eccentricity Predictions from STK with and without the Spherical SRP Model.

The forces experienced at different β angles caused changes to eccentricity. This correlation is demonstrated in **Figure 6**. Maximums and minimums in β, periods of total orbital sunlight, correspond to peaks in eccentricity. In full solar conditions the orbit became more eccentric because solar radiation pressure accelerates and decelerates the sail throughout the entire orbit. Troughs in eccentricity occur at times where β ≈ 0°. In periodic solar conditions the orbit grew circular because the acceleration and deceleration balanced the SRP effect[viii].

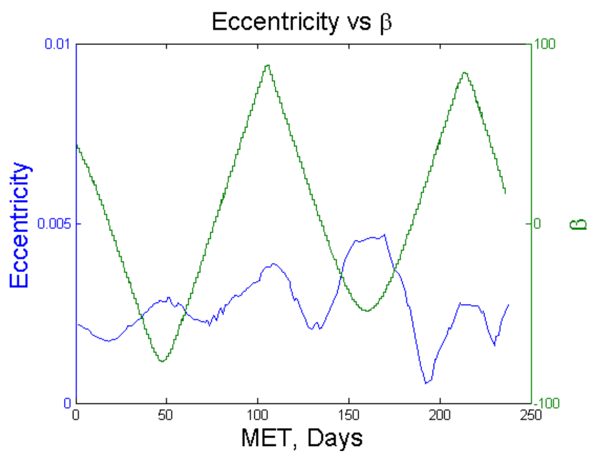

Figure 6. Eccentricity and β Plotted against Mission Elapsed Time in Days

4. METHODS

NSD's attitude moved rapidly over the course of the mission. The changing attitude caused the drag area to similarly fluctuate. An effective drag area was established through the comparison of STK orbital predictions and TLE data. A 3-DOF rigid body dynamics simulation was created in MATLAB to assess attitude stability and to establish upper limits on the solar Center of Pressure (CP) location. By establishing an upper limit for the solar CP, a standard for sail rigidity and symmetry can be postulated for future solar sails in Low Earth Orbit that are similar in design to NSD.

Satellite Tool Kit was used to establish average drag areas of the sail for ten-day periods. STK has a propagator called the High Precision Orbit Propagator (HPOP) that allows high precision calculations of drag. For each ten-day segment of the sail's mission, a probable mass/drag area ratio was selected based on the comparison of STK's predictions and TLE data for NSD as shown in **Figure 7**. STK predictions in blue align with the TLE data in red. This demonstrates that an accurate mass/drag area ratio was selected in HPOP.

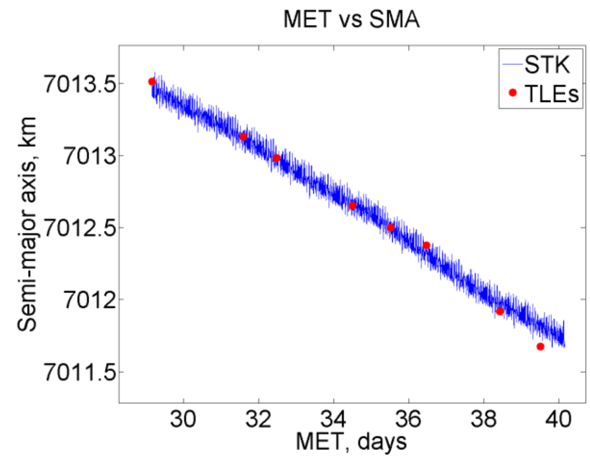

Figure 7. STK and TLE Comparison

The 3-DOF rigid body dynamics model was designed from the equation:

$$I \cdot \alpha + \omega \times (I \cdot \omega) = \tau$$

I is the moment of inertia tensor, α represents the rotation acceleration vector; ω is the angular velocity vector; and τ is the sum of the torques vector. Through torque calculation, the attitude and angular velocity can be integrated.

Aerodynamic drag, solar radiation pressure, and gravity, cause torques on the sail. The torques are calculated by crossing the force vector and the moment arm, which runs from the Center of Gravity to the Center of Pressure. Drag force is calculated through the equation:

$$f_{drag} = \frac{1}{2}\, \rho\, v^2\, Cd\, A$$

The equation illustrates aerodynamic drag's dependency on density ρ, satellite velocity *v*, and *A* – the sail area in drag. *Cd* represents the Co-efficient of drag[ix]. Solar force is calculated through the equation:

$$f_{solar} = \frac{2\, S\, We}{c} \left[\left(\frac{r_e}{r_s} \right)^2 \right]$$

The equation demonstrates that solar force depends on the ratio of the distance of earth from the sun, r_e to the distance of the satellite from the sun, r_s. *S* is the total sail area, *We* is the solar constant equal to 1368 $\frac{J}{sm^2}$, and c is the speed of light.[x] The x, y, and z components of the force of gravity are calculated through the equations:

$$L_x = \frac{3k}{R^3}\left[\left(I_{zz} - I_{yy}\right)a_y a_z\right]$$
$$L_y = \frac{3k}{R^3}\left[\left(I_{xx} - I_{zz}\right)a_z a_x\right]$$
$$L_z = \frac{3k}{R^3}\left[\left(I_{yy} - I_{xx}\right)a_x a_y\right]$$

The variable k is the gravitational constant, R is the Semi-Major Axis; I_{xx}, I_{yy}, I_{zz} are the inertial moments along the x, y, and z axes respectively, and a_x, a_y, and a_z 'are the direction cosines of R with respect to the body frame of the sail'[xi]. L_x, L_y, and L_z combine to form the gravitational torque: L. The gravitational torque equations differ because they depend upon the sail attitude.

5. RESULTS

It was observed that in full lighting the sail converged to a stable attitude. A variety of trade studies examined probable causes of the stability: the effect of initial attitude; the effect of isolated torques; and the effect of an offset Center of Pressure. Also during full sun, NSD is an inertially axisymmetric spacecraft with near-constant disturbance torques, which is a classic condition for a spin-stabilized spacecraft.[xii]

Aerodynamic drag analysis from STK and TLE comparison indicated that NSD-2 experienced drag areas which ranged from 0.69 m^2 to 6.91 m^2 – between 6.9% and 69.1% of the total sail area of 10 m^2. The results of this analysis are displayed in **Figure 8**.

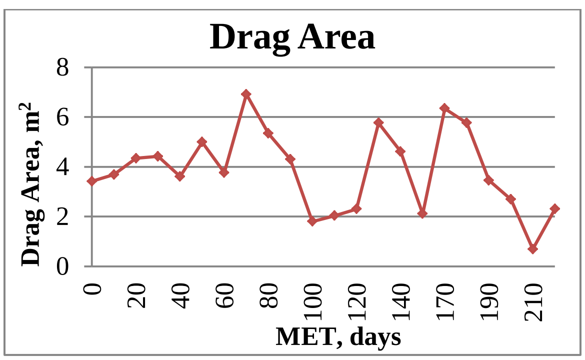

Figure 8. Drag Areas Established through STK and TLE Comparison

The 3-DOF Rigid Body Dynamics simulation was used to perform trials with different variables to understand the causes of the sail's attitude motion. Trade study dates were selected based on the β angle of the sail's orbit. The short time frame of day 41 to 42.7 was selected because this is the first β (-66°) at which the sail begins to experience full sun at all points of the orbit.

In the initial attitude trade study four attitudes were tested: a pitch of 30° and 210° and a roll of 30° and 210°. Pitch and roll are of greater interest than yaw because no torques affect yaw when CP is at the origin. The gravity gradient will affect pitch or roll, while aerodynamic drag will cause pitch changes and solar radiation pressure will cause roll movement. The initial attitude altered the time span for relative stabilization of the sail as shown in **Table 1**. Axial times have been averaged to represent total sail stabilization. Stabilization was defined as the point at which the rate of rotation or the inertial attitude entered a regular (typically sinusoidal) pattern and/or flattened.

Table 1: Initial Attitude Effect on Stabilization

Initial Attitude	Rotation Stabilization Time	Inertial Attitude Stabilization Time
Pitch 30	0.115 days	0.34 days
Pitch 210	0.09 days	0.29 days
Roll 30	0.36 days	0.43 days
Roll 210	0.23 days	0.29 days

Different initial rates were also observed. However, the disturbance torques tended to dominate the initial rates. That is, after a short period of time the simulations tended to converge to a similar state independent of rates. Furthermore, only very limited information on the rate history of the NSD is available (a handful of optical observations) so for the study discussed in Table 1, the initial rotation rate is assumed to be zero.

The torques were simulated individually as well. This served to verify the model and to better examine the ways that each torque affected the sail. The simulation with only a solar torque caused a rapid stabilization of inertial attitude and body rotation rates. This indicates that solar radiation pressure does not tend to cause instability during full sun conditions. **Figure 9a** displays the solar torque effect on inertial attitude. The sail's attitude in the inertial frame stabilizes along all axes at day 41.16 when affected by only solar torque. The final attitude is: [-73.2, -73.2, 90]. **Figure 9b** shows the solar torque effect on sail rotation. Rotation instability was also brief and ended in the roll and pitch axes simultaneously at 41.16 days. In these axes the rotation rate continued to increase and decrease steadily with minimal oscillation, respectively.

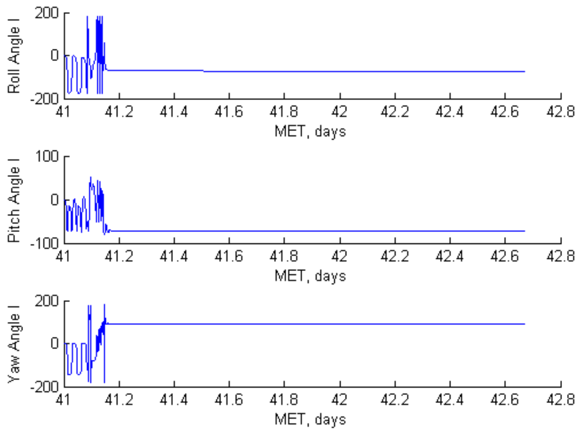

Figure 9a. Solar Torque Effect on Inertial Attitude

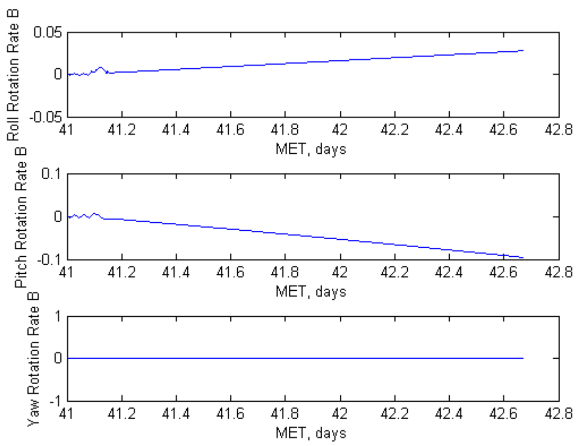

Figure 9b. Solar Torque Effect on Rotation Rates

The simulation with only gravity torque caused longer stabilization time of inertial attitude at 0.14 days from the simulation start at 41 days, displayed in **Figure 10a**. Minimal oscillations continued in the pitch axis. The sail stabilized at the attitude: [87.4, -87.4, -90] Gravity caused more disturbance of the rotation rates than solar torque. This is evident in the regular oscillations in the roll rotation rate shown in **Figure 10b**. Gravity caused unstable rotation in the roll axis for 0.1 days, then regular oscillations resumed and the overall rate of rotation became negative. In the pitch axis minimal oscillation controlled rotation for the complete analysis segment. The graphs show that gravity is responsible for minimal oscillation within an orbit in full sunlight.

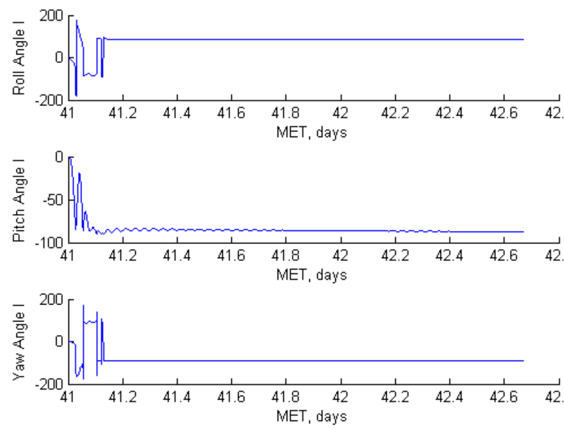

Figure 10a. Gravity Effect on Inertial Attitude

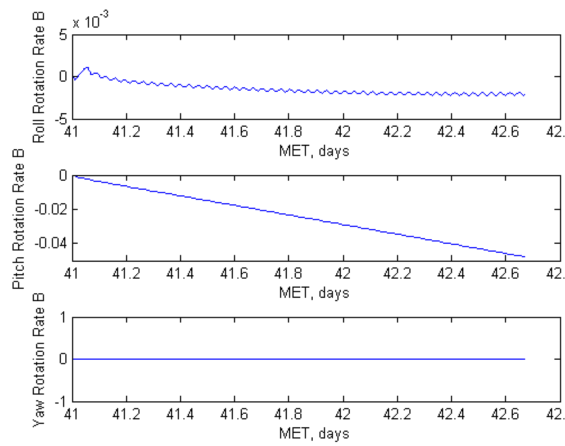

Figure 10b. Gravity Effect on Rotation Rates

The simulation with only aerodynamic drag caused instability in the sail. In the inertial frame the sail showed small trends towards stability at approximately 42.6 days in the roll and pitch axes, as seen in **Figure 11a**. When aerodynamic drag is present, the sail does not fully stabilize within 1.7 days. The sail rotates with no regularity in the roll and pitch axes, shown in **Figure 11b**. The rotation rates do not present any regularity or stability when only drag affects the sail.

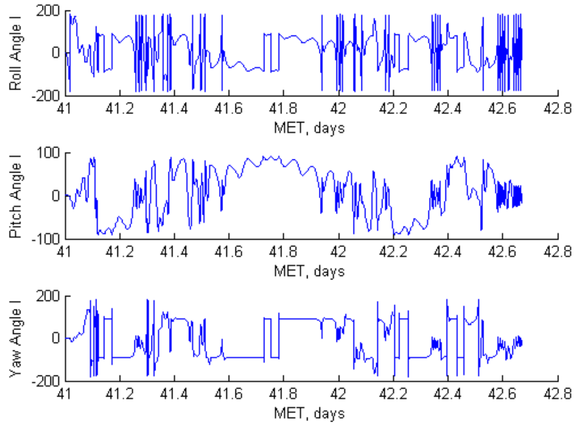

Figure 11a. Drag Torque Effect on Inertial Attitude

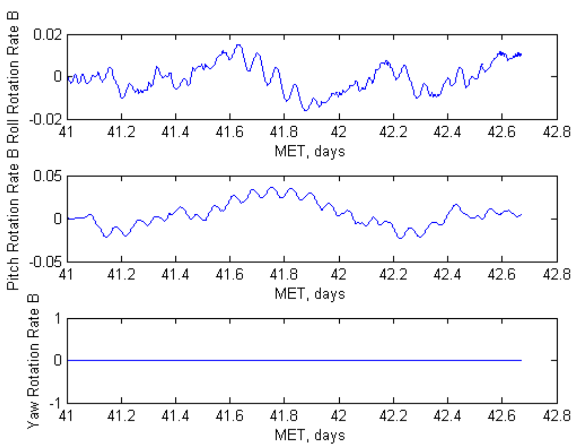

Figure 11b. Drag Torque Effect on Rotation Rate

Since drag did not stabilize in the initial study time span, another long range (approximately ten-day) study was conducted. The results showed that when the sail is affected by aerodynamic drag, the sail remains unstable for the extended analysis period.

A trade study on the solar Center of Pressure (CP) effects was conducted to establish an upper limit of the solar CP offset in the sail plane. Given the symmetry of the sail, the initial assumption is that CP is at the geometric center of the sail, but this is almost certainly not true due to manufacturing defects and exposure to the environment. The torques are calculated from the vector from the Center of Gravity to the point of force contact at the CP. Changes to the CP were only evaluated along the X and Y-axes because a change to the Z-axis point of contact is prohibited by design. (Alternate CG values along the Z axis were considered in a separate study but that is beyond the scope of this paper).

For the first sample offset, 0.001 m.., major stabilization was achieved in 0.36 days in the inertial frame, shown in **Figure 12a**. Small oscillations continue for the course of analysis. The rotation rate in **Figure 12b** also stabilizes quickly with regular and minute oscillations at an offset of 0.001 m. Of note, there is yaw rotation in an offset CP situation. In most cases the sail does not rotate about the yaw axis.

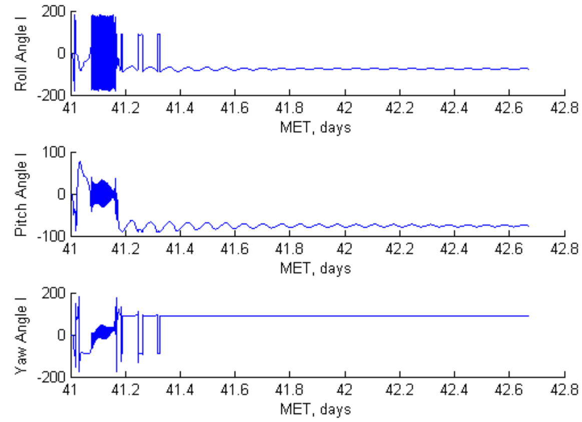

Figure 12a. Inertial Attitude for 0.001 m. CP Offset

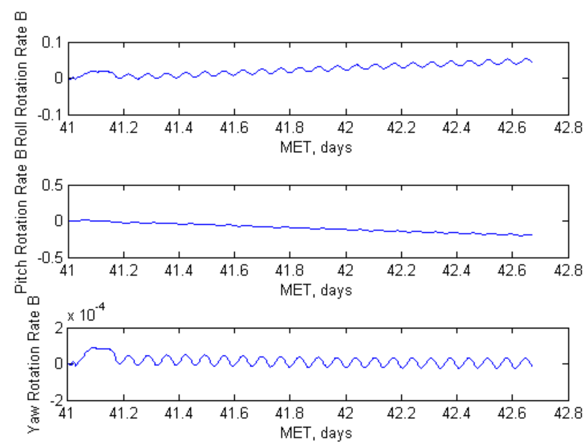

Figure 12b. Rotation Rate for 0.001 m. CP Offset

When the CP offset was 0.005 m. the sail primarily stabilized at 42.16 days, 1.16 days into the analysis, as seen in **Figure 13a**. This stabilization time was three times slower than for an offset of 0.001 m. The rotation rate was less disturbed by the offset and stabilized in 0.1 days, shown in **Figure 13b**.

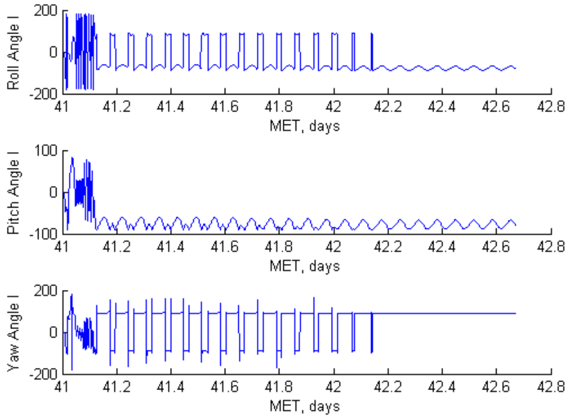

Figure 13a. Inertial Attitude for 0.005 m. CP Offset

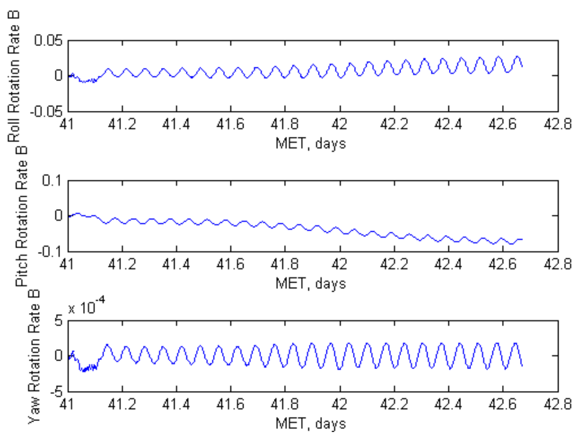

Figure 13b. Rotation Rate for 0.005 m. CP Offset

For the largest offset studied, 0.05 m., the sail did not show stabilization signs over the 1.7-day analysis segment in attitude or in rotation rates. The inertial attitude results are shown below in **Figure 14a** and the rotation rate results are shown in **Figure 14b**.

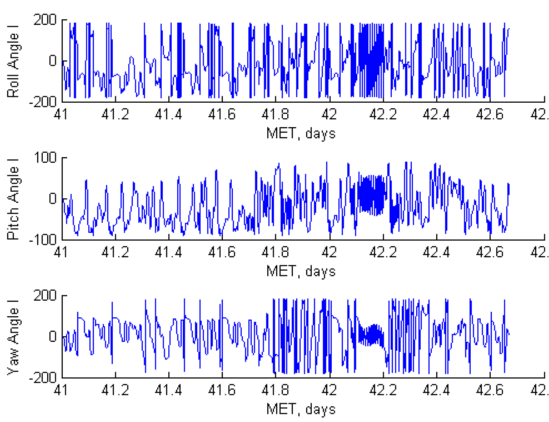

Figure 14a. Inertial Attitude for 0.05 m. CP Offset

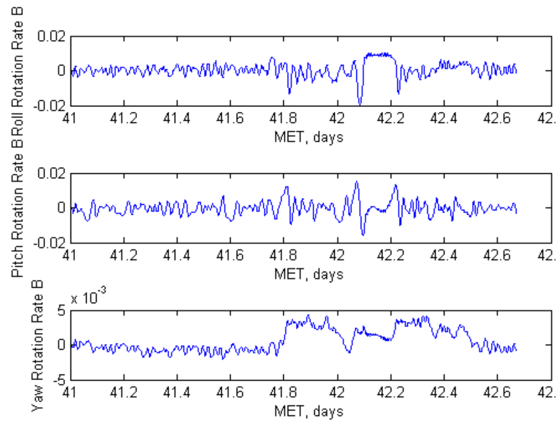

Figure 14b. Rotation Rate for a 0.05 m. CP Offset

The CP offset analysis demonstrates that the sail will tend to remain stable when there are small offsets in the X-Y plane. Instability would dominate any restoring forces if the offset exceeded 0.05 m. Offsets less than 1 cm. increase the stabilization time, but do not completely impede stabilization.

6. CONCLUSION

When the sail orbits in full sun, near a maximum or minimum β, the sail tends to orbit in a stable attitude. Thus, if a future solar sail is again deployed in Low Earth Orbit as a demonstration, the ideal orbit would be full sun, such as a polar sun-synchronous orbit.

The Center of Pressure is critically important to the sail's stability. If the CP offset in the sail plane from the CG is too large, it will prohibit sail stabilization. This means that Low Earth Orbit sails need rigid structures that permit little to no flexibility in the Center of Pressure. This also implies that the CG location should be carefully measured pre-mission and that future missions should be prepared to estimate CP from flight data in a rigorous fashion.

Changes in initial attitude did not affect the sail's ability to stabilize at high values of β. The initial attitude did alter the final attitude at which the sail precessed about at approximately a 1° cone angle.

Studies indicate that drag has a strong effect on the sail's stability. Sail attachment to another satellite may be unstable. Solar torques and gravity torques limit these effects. Otherwise active controls of sail attitude may prove necessary for deorbit missions with solar sails.

The use of sails as deorbit devices for space debris is promising. The high drag area caused the sail to deorbit in ~9 months. The majority of Low Earth

Orbit debris would naturally deorbit over the course of years. An increased drag area from a solar sail would cause the junk to deorbit rapidly. The mission also demonstrated that a sail is feasibly deorbited via a cube satellite.

A critical finding of this research is that orbit data and attitude dynamics simulations agree that during full sun conditions NSD achieved spin stability typical of an axisymmetric spacecraft with a constant torque. This result provides valuable insight for future sails that may want to deploy into Low Earth Orbit.

In future research, the sail model needs to be updated to accurately model the SRP effect of the satellite shell which originally housed the sail. The cube was 10 cm. x 10 cm. x 30 cm. The omission of this component of the model may lead to minimal inaccuracies in the drag effect on the sail. It should not have altered the gravity effect or the solar pressure effect because gravity is dependent upon sail attitude and SRP would create minimal disturbances only when the sail did not shadow the cube. Given the small dimensions of the satellite shell relative to the sail area the solar effect is negligible. The drag caused by the shell is likely to be the strongest disturbance. It is important to more fully investigate this to know its effect on sails' capacity to deorbit space debris.

ACKNOWLEDGEMENTS

Andrew F. Heaton of EV42 at NASA Marshall Space Flight Center for his mentorship and considerable aid in the research presented.

REFERENCES

[i] Orbital Debris, Frequently Asked Questions. (March, 2012). *NASA Orbital Debris Program Office*. April 16, 2012. http://orbitaldebris.jsc.nasa.gov/faqs.html .

[ii] Orbital Debris, Graphics. (April 29, 2005). *NASA Orbital Debris Program Office*. April 15, 2012. http://orbitaldebris.jsc.nasa.gov/photogallery/beehives.html#geo .

[iii] Whorton, Mark. (August, 2008). *NanoSail-D: The First Flight Demonstration of Solar Sails for Nanosatellites*. AIAA/USU Conference on Small Satellites, Logan, Utah.

[iv] Alhorn, Dean. (August, 2011). *NanoSail-D: The Small Satellite That Could!* AIAA/USU Conference on Small Satellites, Logan, Utah.

[v] Whorton, Mark. (August, 2008). *NanoSail-D: The First Flight Demonstration of Solar Sails for Nanosatellites*. AIAA/USU Conference on Small Satellites, Logan, Utah.

[vi] Alhorn, Dean. (August, 2011). *NanoSail-D: The Small Satellite That Could!* AIAA/USU Conference on Small Satellites, Logan, Utah.

[vii] Vallado, David A. (2007). *Fundamentals of Astrodynamics and Applications*. New York, NY. Springer.

[viii] Lücking, Charlotte. (2011). *A Passive High Altitude Deorbiting Strategy*. AIAA/USU Conference on Small Satellites, Logan, Utah.

[ix] Bate, Roger R., Mueller D. D. & White, J. E. (1971). *Fundamentals of Astrodynamics*. New York: Dover Publications.

[x] McInnes, Colin. (1999). *Solar Sailing: Technology, Dynamics and Mission Applications*. Chichester, UK: Praxis Publishing Ltd.

[xi] Harris, Mark. (May, 1969). *Spacecraft Gravitational Torques*. National Aeronautics and Space Administration. Langley, VA. NASA-SP 8024.

[xii] Wertz, James R. (Ed). (1978). *Spacecraft Attitude Determination and Control*. Hingham, MA. D. Reidel Publishing Company, Inc.